Supplementary Information for

Theoretical Elucidation of Water-Mediated Multiple Proton Transport in the Sulfonates

Longda Wei[a#], Yitong Zhu[a#], Jiasheng Wang[a], Weiwei Zeng[a], Chengkun Zhou[a], Yuqing, Yan[a,*], Bo Li[a,*], Jingping Zhang[b,*]

[a]*Hebei Key Laboratory of Hazardous Chemicals Safety and Control Technology, School of Chemical Safety, North China Institute of Science and Technology, Langfang 065201, Hebei, China*
[b]*Faculty of Chemistry, Northeast Normal University, Changchun 130024, Jilin, China*
[#]Longda Wei and Yitong Zhu are co-first authors.
[*]Corresponding authors.
E-mail addresses: yanyq80@163.com (Y.Q.Yan); libo@ncist.edu.cn (B. Li); zhangjp162@nenu.edu.cn (J.P. Zhang).

3. IRC calculation data.

4. Vibrational Circular Dichroism spectroscopy

5. Infrared spectroscopy

6. Raman spectroscopy

7. Ultraviolet-Visible Absorption Spectrum

8. ^{1}H-NMR spectrum

1. Methods and Proton Transport Mechanism

All calculations were carried out with Gaussian 16 series of programs (Revision C.01). Geometry optimizations, single point energy, NPA, frequency and excited states were performed with the density functional theory (DFT) M06-2X-D3 method (the hybrid meta density functional theory M06-2X recently developed by Truhlar and co-workers has shown its efficiency and accuracy in predicting properties for the main-group thermochemistry and kinetics) coupled with the def2-TZVP basis set (polarization functions are added to the hydrogen to render the final energies accurate).

The dynamic processes of the proton transfer are carried out with flexible potential energy surface (PES) scans of the title proton and the oxygen bond length. The energy maximum occurs at c.a. 2 Å between the title proton and oxygen atoms. Vibration (IR, Raman, and VCD) and electronic spectra (UV-Vis), NPA and NMR chemical shifts were calculated using single-point energy computations at the optimized geometries of three critical configurations: the reactant state, the transition state, and the product state.

Natural Population Analysis (NPA), rooted in Löwdin orthogonalization and natural atomic orbital (NAO) theory, provides a robust framework for quantifying atomic charges and bond orders by partitioning electron density into chemically meaningful components. Unlike Mulliken analysis, NPA mitigates basis-set artifacts through NAO transformation, delivering reliable charge distributions (e.g., $\Delta q > 0.2e$ in proton-transfer systems) that align with spectroscopic data (IR, NMR) and reaction energetics. Recent advancements highlight its role in machine-learned force fields (Smith et al., J. Chem. Theory Comput. 2023, 19, 5123–5136) and electrocatalyst

design (Zhang et al., Nat. Catal. 2024, 7, 231–245), where NPA-derived charges validate DFT-predicted active sites. The method's synergy with ab initio molecular dynamics (AIMD) further bridges electronic structure and macroscopic properties, as demonstrated in proton-conducting polymers (Lee & Hynes, Chem. Rev. 2025, 125, 10288–10320).

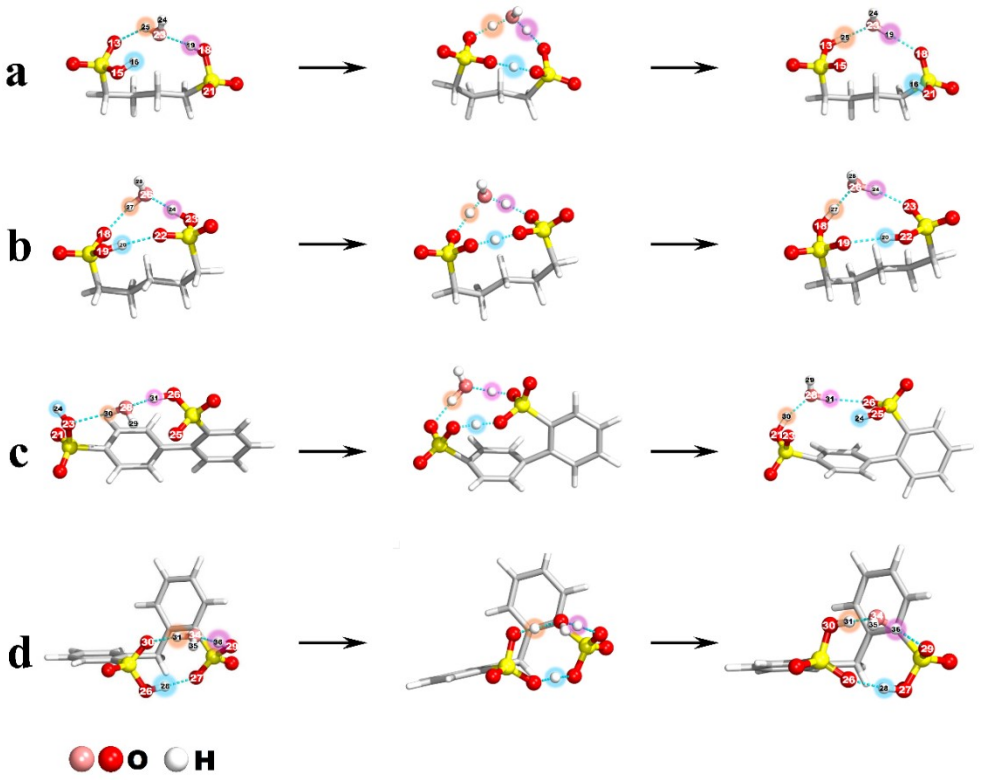

Supplementary Figure S1| TPSH processes in BDS-1W, PDS-1W, BPS-1W, and MDBS-1W：(a) for *Butanedisulfonic* acid-1 water; (b) for *Pentanedisulfonic* acid-1 water; (c) for *2-(3-sulfophenyl)benzenesulfonic* acid-1water;(d) for *4,4'-Methylenedibenzenesulfonic* acid-1 waters.

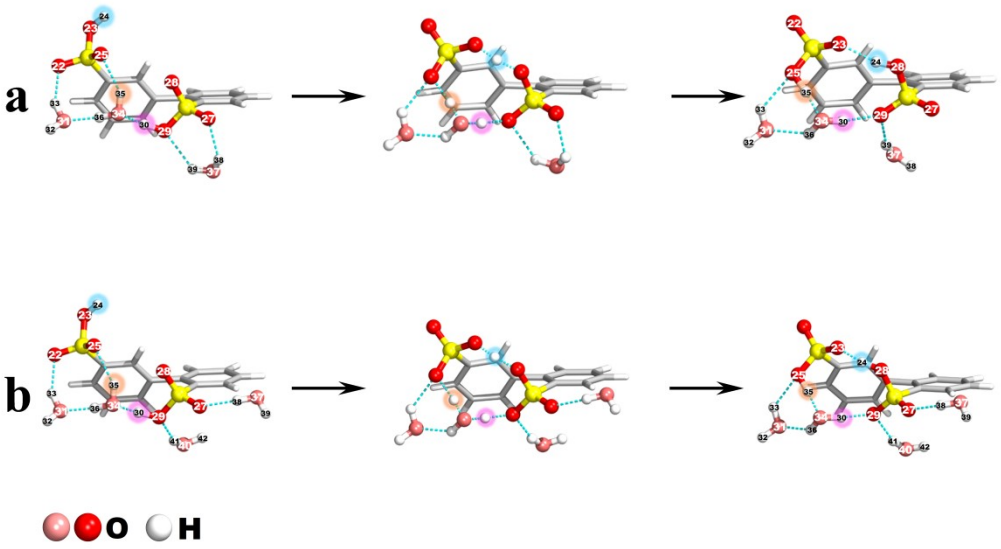

Supplementary Figure S2| The proton transfer processes of 3,3'-biphenyldisulfonic acid-(3-4) water compounds (E_a = 0.2639 eV) with the numbering scheme: (a) for 3,3'-biphenyldisulfonic acid-3 waters; (b) for 3,3'-biphenyldisulfonic acid-4 water (E_a = 0.2656 eV).

Supplementary Table S1| The activation energies of MBS-0W, MBS-1W, MBS-2W, BPD-0W, BPD-1W, and BPD-2W in vacuum and considering water solvent effect.

	Vacuum (ε = 1)	Water (ε = 78.5)
MBS-0W	2.340 eV	1.950 eV
MBS-1W	1.530 eV	1.540 eV
MBS-2W	1.370 eV	1.340 eV
BPD-0W	0.339 eV	0.763 eV
BPD-1W	0.287 eV	0.119 eV
BPD-2W	0.269 eV	0.112 eV

2. Transition state data

Supplementary Table S2| Imaginary frequencies for the MBS-1W, MBS-2W, BPD-0W, BPD-1W, and BPD-2W models.

	Frequencies(cm^{-1})
MBS-1W	-1009.66
MBS-2W	-994.28
BPD-0W	-512.14
BPD-1W	-705.46

	Frequencies(cm^{-1})
BPD-2W	-725.00

Supplementary Table S3| Relax scan parameters for the MBS-0W, MBS-1W, MBS-2W, BPD-0W, BPD-1W, and BPD-2W models

	MBS-0W	MBS-**1**W	MBS-**2**W	BPD-0W	BPD-1W	BPD-2W
Step Size(Å)	0.05	0.05	0.05	0.05	0.05	0.05
Range(Å)	5.463	5.238	5.337	1.984	4.050	4.838
Scanned Coordinates	H20-O13	H20-O13	H20-O13	H24-O28	H24-O28	H24-O28
Scan Type	relax	relax	relax	relax	relax	relax

Supplementary Table S4| Calculation of single-point energies for the initial states, transition states, and final states of the MBS-0W, MBS-1W, MBS-2W, BPD-0W, BPD-1W, and BPD-2W models using the DLPNO-CCSD（T）method.

	MBS-0W	MBS-1W	MBS-2W
IS（Hartree）	-1478.048223405267	-1554.404530178425	-1630.762905701347
TS（Hartree）	-1477.948320929152	-1554.341600084139	-1630.704393477061
FS（Hartree）	-1477.954000474080	-1554.404744178347	-1630.761152952537
Energy Barrier（eV)	2.718 eV	1.712 eV	1.592 eV
Meth	DLPNO-CCSD(T)	DLPNO-CCSD(T)	DLPNO-CCSD(T)

	BPD-0W	BPD-1W	BPD-2W
IS（Hartree）	-1708.669087444684	-1785.031019477770	-1861.384932288002
TS（Hartree）	-1708.652973684347	-1785.015848310979	-1861.369897198179
FS（Hartree）	-1708.671622980602	-1785.035030272660	-1861.375957050705
Energy Barrier（eV)	0.435 eV	0.413 eV	0.409 eV
Meth	DLPNO-CCSD(T)	DLPNO-CCSD(T)	DLPNO-CCSD(T)

Supplementary Table S5| Calculation of single-point energies for the initial states, transition states, and final states of the MBS-0W, MBS-1W, MBS-2W, BPD-0W, BPD-1W, and BPD-2W models using the MP2 method.

	MBS-0W	MBS-1W	MBS-2W
IS（Hartree）	-1477.924604106681	-1554.268833479557	-1630.614926215494
TS（Hartree）	-1477.827448058598	-1554.213085115817	-1630.563427200787
FS（Hartree）	-1477.833437198010	-1554.268608272593	-1630.613116084168

Energy Barrier（eV)	2.644 eV	1.401 eV	1.592 eV
Meth	MP2	MP2	MP2

	BPD-0W	BPD-1W	BPD-2W
IS（Hartree）	-1708.489819560220	-1784.838699391149	-1861.180215996608
TS（Hartree）	-1708.476954127193	-1784.828579657071	-1861.169748012669
FS（Hartree）	-1708.492064741064	-1784.843666898447	-1861.173938101950
Energy Barrier（eV)	0.350 eV	0.275 eV	0.285 eV
Meth	MP2	MP2	MP2

Supplementary Table S6| Calculation of energy barriers using DLPNO-CCSD(T), MP2, and M06-2X methods for the MBS-0W, MBS-1W, MBS-2W, BPD-0W, BPD-1W, and BPD-2W systems.

	M06-2X	MP2	DLPNO-CCSD(T)
MBS-0W	2.339 eV	2.644 eV	2.718 eV
MBS-1W	1.534 eV	1.401 eV	1.712 eV
MBS-2W	1.526 eV	1.592 eV	1.592 eV
BPD-0W	0.339 eV	0.350 eV	0.435 eV
BPD-1W	0.287 eV	0.275 eV	0.413 eV
BPD-2W	0.269 eV	0.285 eV	0.409 eV

Supplementary Table S7| Hydrogen bond lengths in the MBS-1W system at the initial state (IS), transition state (TS), and final state (FS).

MBS-1W	IS (Å)	TS (Å)	FS (Å)
H20-O19		1.22	5.48
H20-O13	5.48	1.22	
H22-O18	3.69	1.39	
H22-O21		1.08	1.69
H17-O21	1.69	1.08	
H17-O16		1.39	3.70

Supplementary Table S8| Hydrogen bond lengths in the MBS-2W system at the initial state (IS), transition state (TS), and final state (FS).

MBS-2W	IS (Å)	TS1 (Å)	FS (Å)
H20-O19		1.25	1.48
H20-O13	6.04	1.20	1.05
H26-O18	1.86	1.55	1.48
H23-O24	1.73	1.31	1.18
H23-O21		1.10	1.21
H17-O21	1.50	1.05	
H26-O24			1.05
H17-O16		1.44	1.52

MBS-2W	IS (Å)	TS2 (Å)	FS (Å)

H20-O19	1.48	1.48	1.92
H20-O13	1.05	1.05	
H26-O18	1.48	1.48	
H26-O24	1.05	1.05	1.42
H23-O24	1.18	1.18	
H23-O21	1.21	1.21	1.61
H17-O16	1.52	1.52	1.82

Supplementary Table S9| Hydrogen bond lengths in the BPD-0W system at the initial state (IS), transition state (TS), and final state (FS).

BPD-0W	IS (Å)	TS (Å)	FS (Å)
H24-O23	1.83	1.12	
H24-O28		1.32	1.98
H30-O25		1.13	1.84
H30-O29	1.96	1.31	

Supplementary Table S10| Hydrogen bond lengths in the BPD-1W system at the initial state (IS), transition state (TS), and final state (FS).

BPD-1W	IS (Å)	TS (Å)	FS (Å)
H24-O23	1.99	1.18	
H24-O28		1.24	2.54
H32-O25		1.29	3.20
H32-O31	1.53	1.13	
H30-O31		1.06	1.49
H30-O29	2.46	1.42	

Supplementary Table S11| Hydrogen bond lengths in the BPD-2W system at the initial state (IS), transition state (TS), and final state (FS).

BPD-2W	IS (Å)	TS (Å)	FS (Å)
H24-O23		1.21	1.51
H24-O28	4.84	1.20	
H35-O25	2.23	1.48	
H35-O34		1.04	1.31
H30-O34	1.46	1.06	
H30-O29		1.40	1.76

Supplementary Table S12| Zero-point energy (ZPE) corrected activation energies (eV) for MBS and BPD systems.

	MBS-0W	MBS-1W	MBS-2W
IS（Hartree）	-1479.830580	-1556.255043	-1632.680443
TS（Hartree）	-1479.736419	-1556.204936	-1632.635450
FS（Hartree）	-1479.756950	-1556.255043	-1632.678986
Energy Barrier（eV)	2.562eV	1.363 eV	1.224 eV

	BPD-0W	BPD-1W	BPD-2W
IS（Hartree）	-1710.795325	-1787.226351	-1863.644134
TS（Hartree）	-1710.787161	-1787.220870	-1863.639038
FS（Hartree）	-1710.793150	-1787.225068	-1863.641365
Energy Barrier（eV)	0.222 eV	0.149 eV	0.139 eV

System	*E*a (uncorrected)	*E*a (ZPE-corrected)	Δ*E*a
MBS-0W	2.339eV	2.562eV	-0.223eV
MBS-1W	1.534 eV	1.363 eV	0.171 eV
MBS-2W	1.371 eV	1.224 eV	0.147 eV
BPD-0W	0.339 eV	0.222 eV	0.117 eV
BPD-1W	0.287 eV	0.149 eV	0.138 eV
BPD-2W	0.269 eV	0.139 eV	0.130 eV

Supplementary Table S13| Gibbs free energy barriers ($\Delta G^{\ddagger}$) and calculated proton transfer rate constants (k) at 298.15 K for all studied systems.

System	$\Delta G^{\ddagger}(eV)$	$\Delta G^{\ddagger}(kJ/mol)$	$\exp(-\Delta G‡/RT)$	$k(\mathrm{s}^{-1})$
MBS-0W	2.339	225.7	2.6×10^{-40}	1.6×10^{-27}
MBS-1W	1.534	148.0	1.1×10^{-26}	6.8×10^{-14}
MBS-2W	1.371	132.3	2.2×10^{-24}	1.4×10^{-11}
BPD-0W	0.339	32.7	1.85×10^{-6}	1.15×10^{7}
BPD-1W	0.287	27.7	1.41×10^{-5}	8.75×10^{7}
BPD-2W	0.269	25.9	2.85×10^{-5}	1.77×10^{8}

Note: $RT = 0.0257$ eV at 298.15 K; $k_B T/h = 6.21 \times 10^{12}$ s^{-1}

3. IRC calculation data.

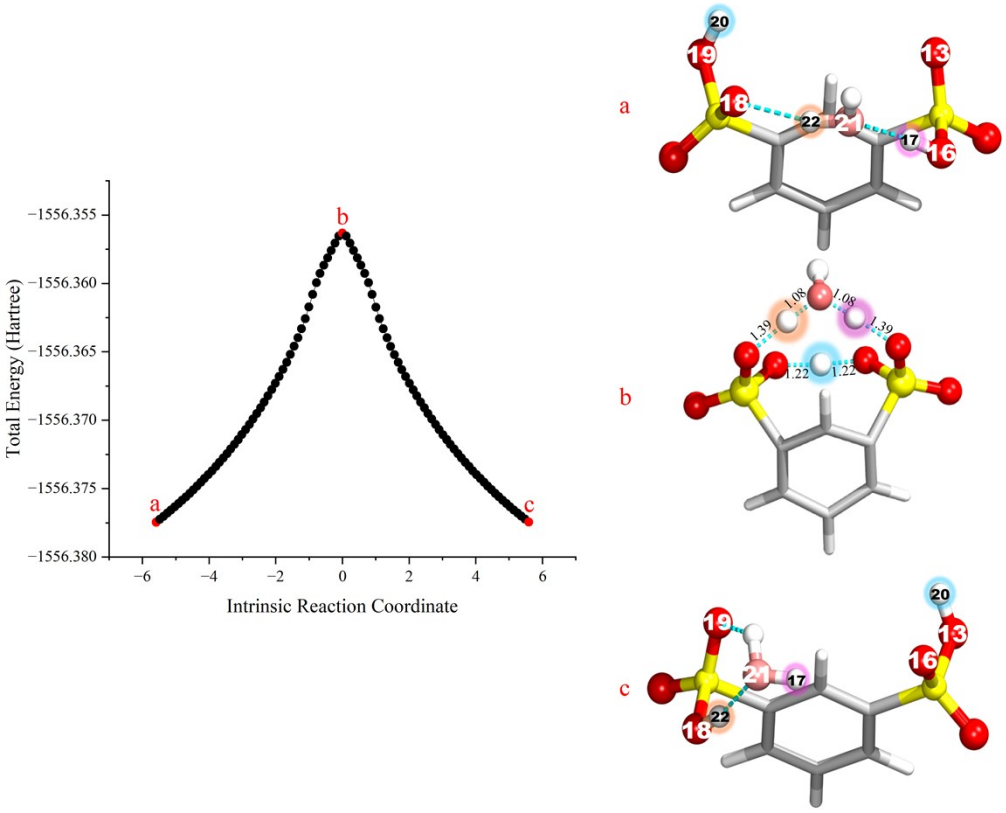

Supplementary Figure S3| MBS-1W models IRC calculation data and optimized initial and final states. a is the initial state, b is the transition state, and c is the final state. The blue dashed line represents the hydrogen bond.

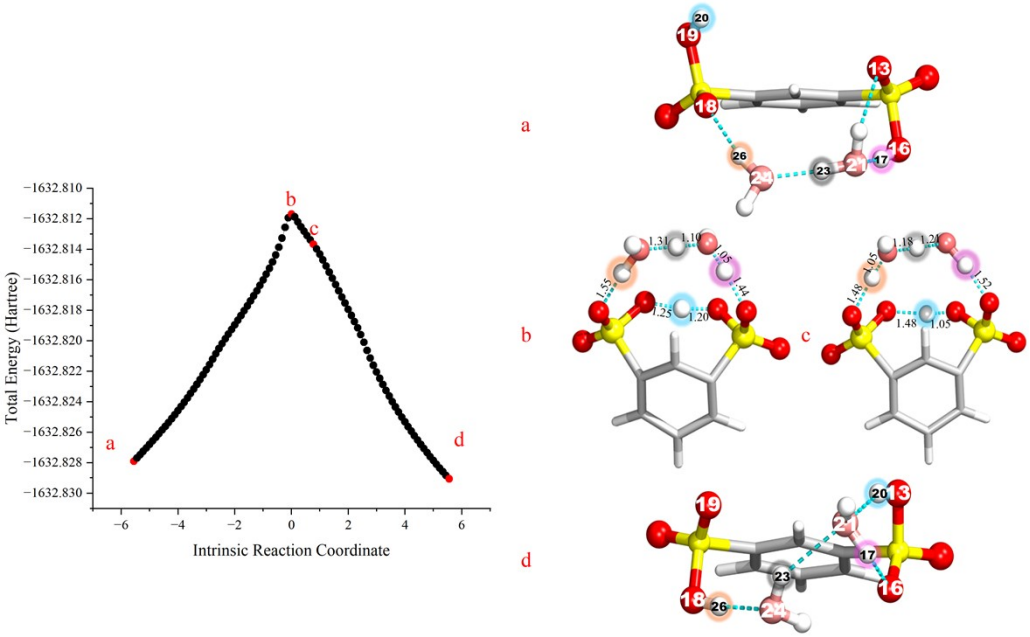

Supplementary Figure S4| MBS-2W models IRC calculation data and optimized initial and final states. a is the initial state, b is the transition state, and c is the final state. The blue dashed line represents the hydrogen bond.

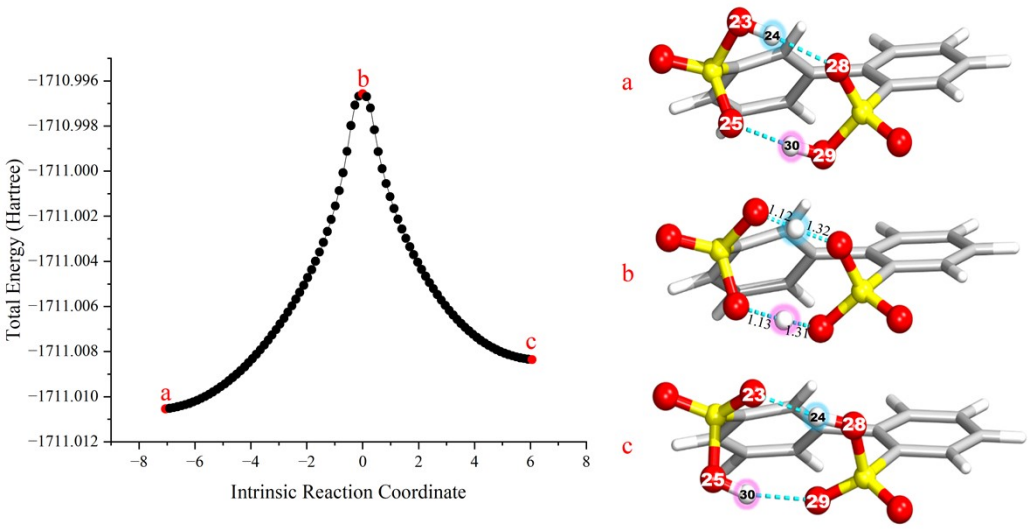

Supplementary Figure S5| BPD-0W models IRC calculation data and optimized initial and final states. a is the initial state, b is the transition state, and c is the final state. The blue dashed line represents the hydrogen bond.

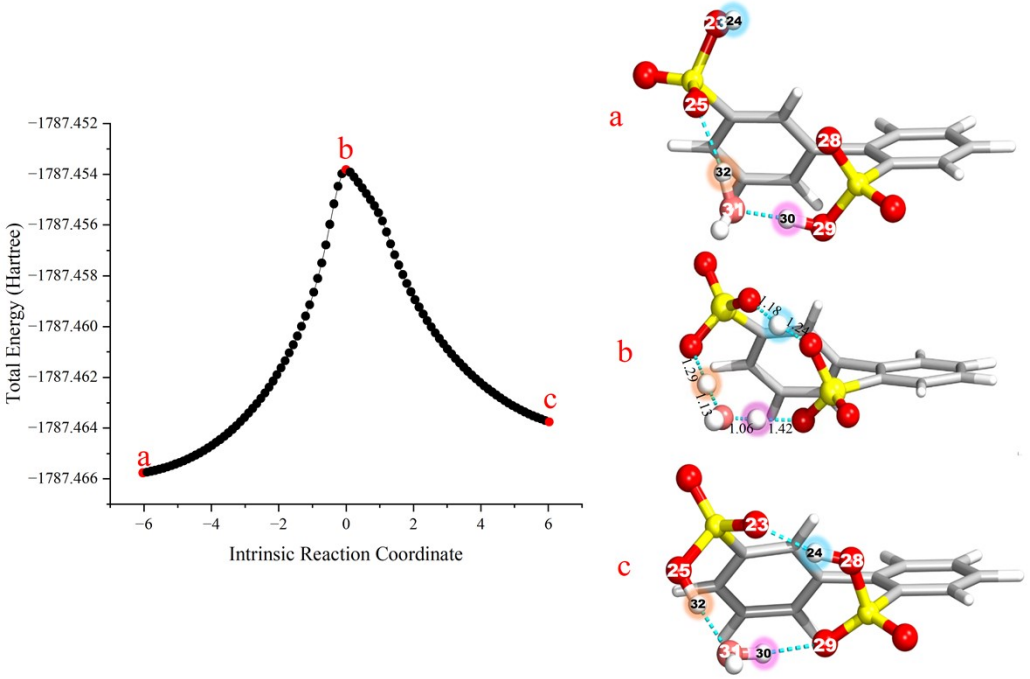

Supplementary Figure S6| BPD-1W models IRC calculation data and optimized initial and final states. a is the initial state, b is the transition state, and c is the final state. The blue dashed line represents the hydrogen bond.

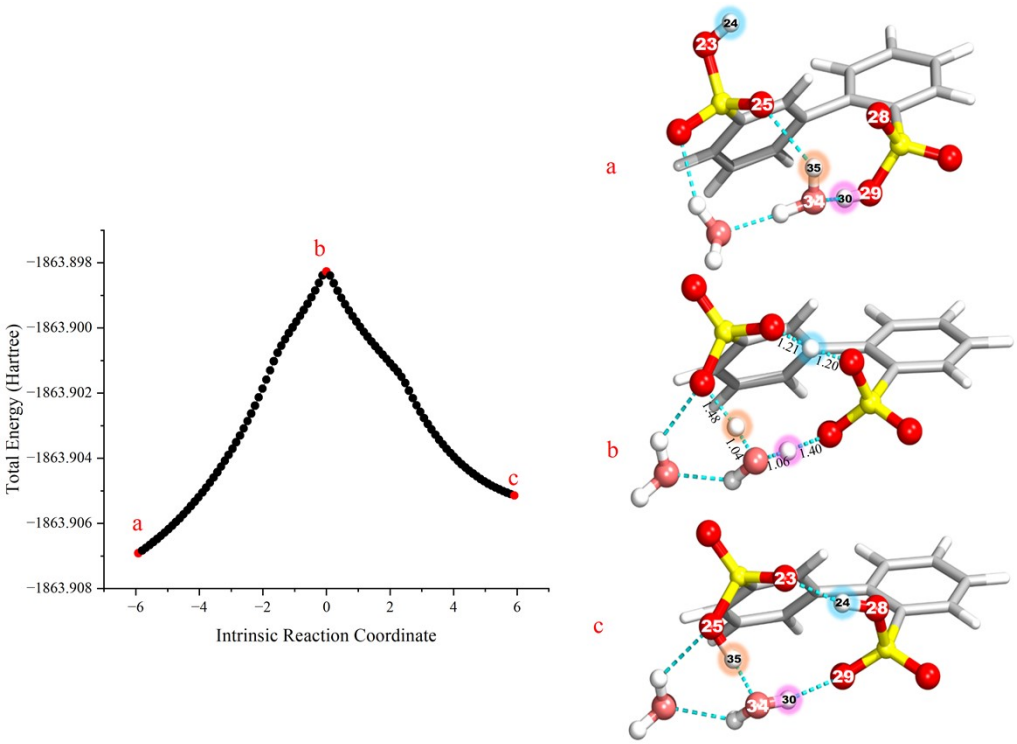

Supplementary Figure S7| BPD-2W models IRC calculation data and optimized initial and final states. a is the initial state, b is the transition state, and c is the final state. The blue dashed line represents the hydrogen bond.

4. Vibrational Circular Dichroism spectroscopy

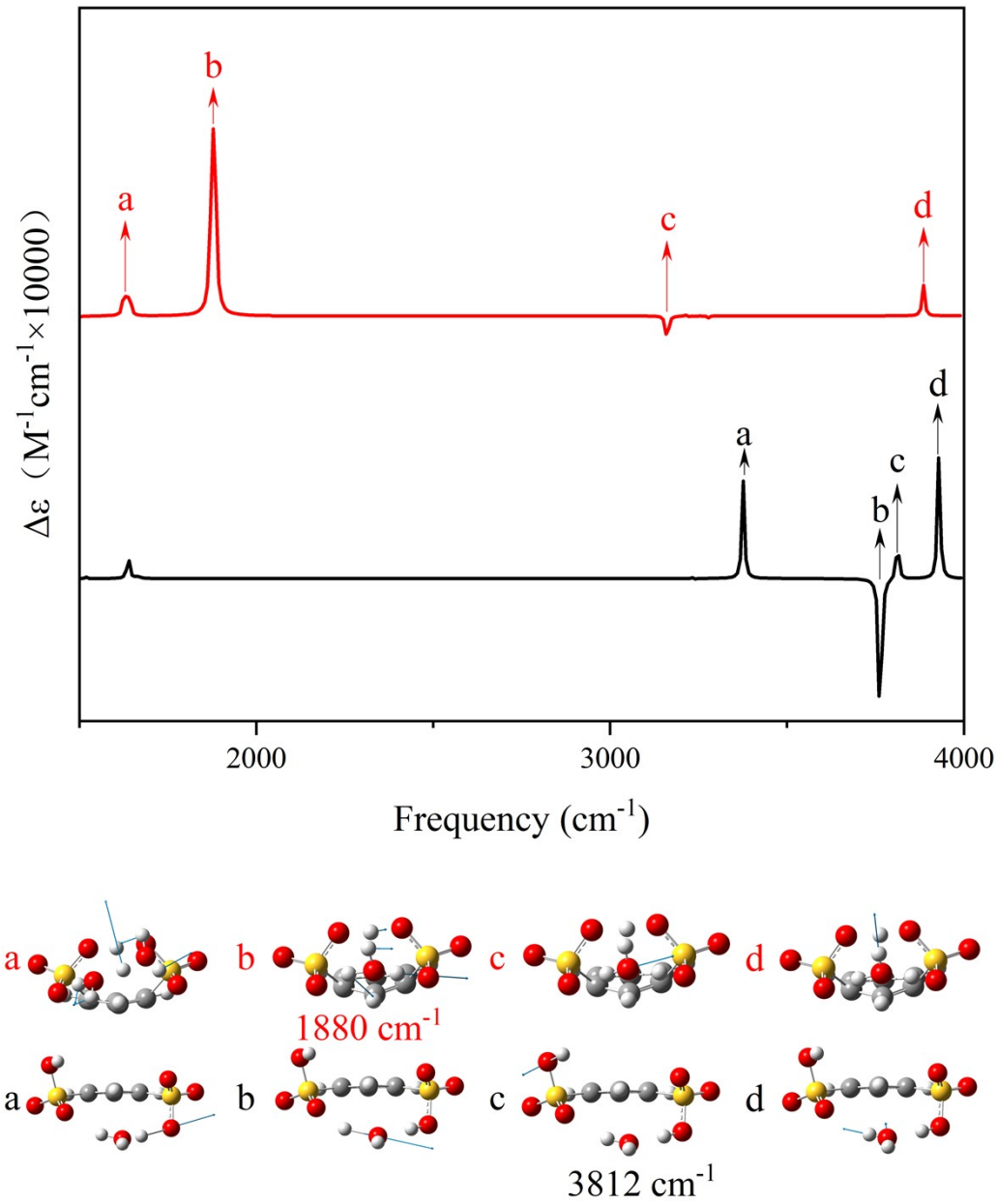

Supplementary Figure S8|Vibrational Circular Dichroism spectroscopy of MBS-1W. Black lines represent the ground state, and red lines represent the proton transition state. The red a and b correspond to the vibrational modes of the transition state peaks, while the black a and b correspond to the vibrational modes of the initial state peaks. The peak at 3812 cm^{-1} corresponds to the stretching vibration of H20-O19 in the initial state, while the peak at 1880 cm^{-1} corresponds to the stretching vibration of H20-O19 in the transition state.

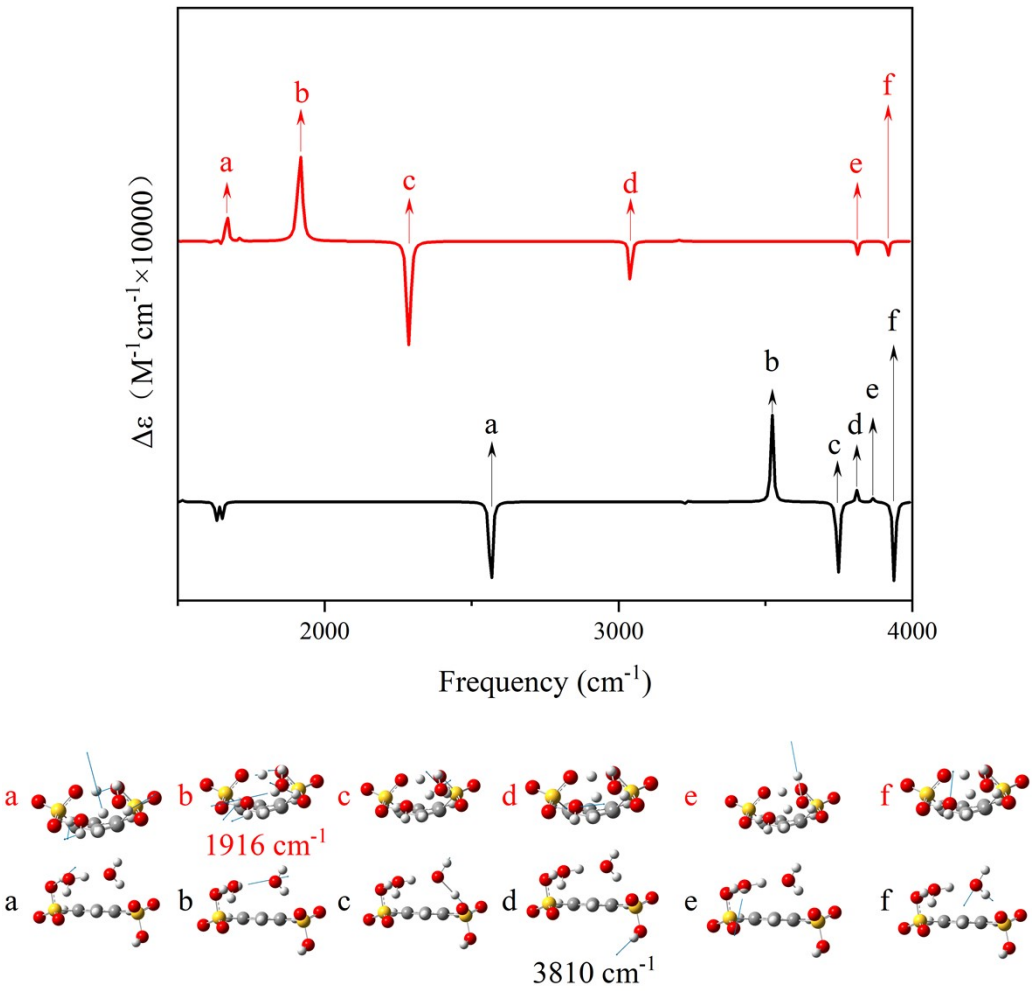

Supplementary Figure S9|Vibrational Circular Dichroism spectroscopy of MBS-2W. Black lines represent the ground state, and red lines represent the proton transition state. The red a and b correspond to the vibrational modes of the transition state peaks, while the black a and b correspond to the vibrational modes of the initial state peaks. The peak at 3810 cm^{-1} corresponds to the stretching vibration of H20-O19 in the initial state, while the peak at 1916 cm^{-1} corresponds to the stretching vibration of H20-O19 in the transition state.

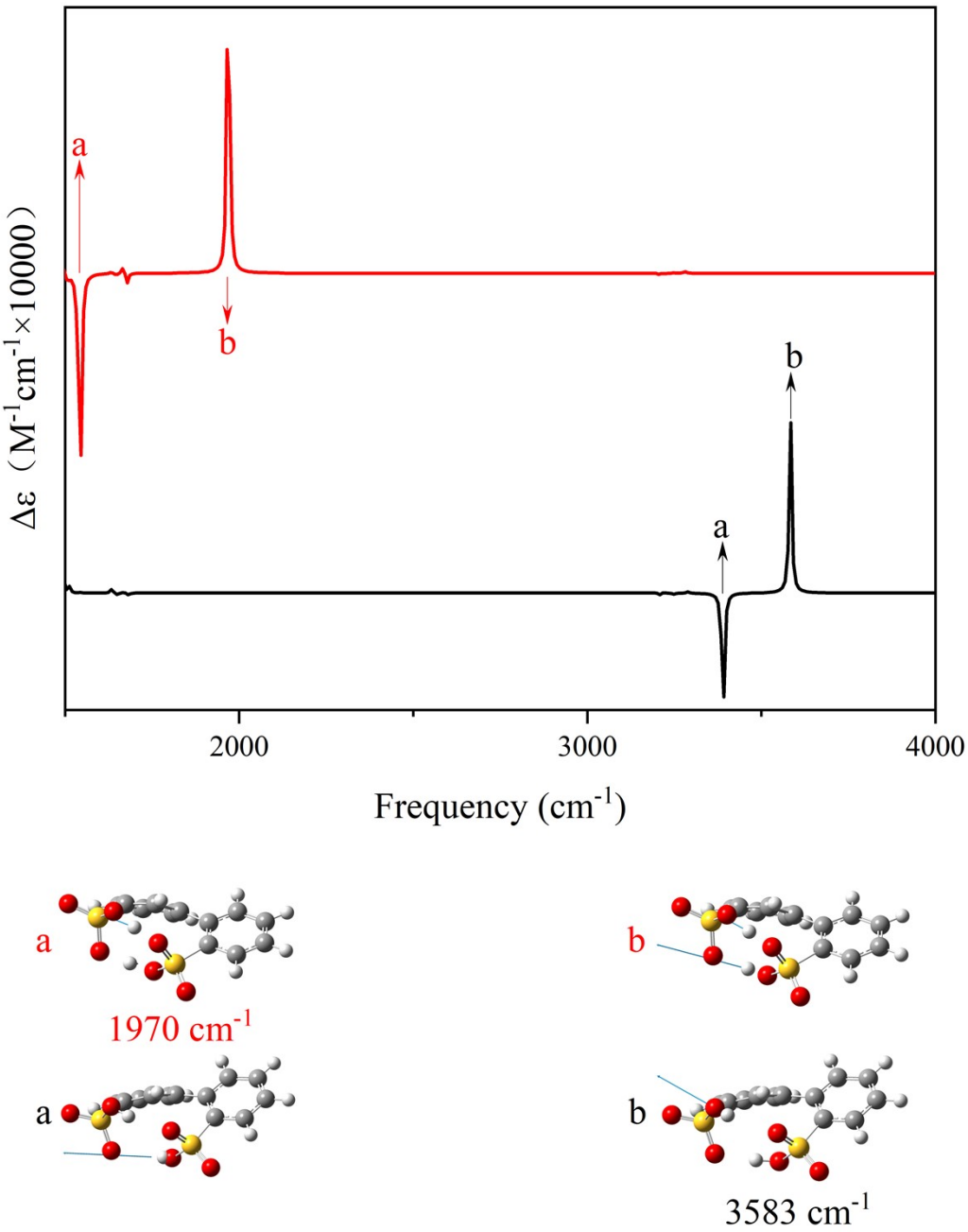

Supplementary Figure S10|Vibrational Circular Dichroism spectroscopy of BPD-0W. Black lines represent the ground state, and red lines represent the proton transition state. The red a and b correspond to the vibrational modes of the transition state peaks, while the black a and b correspond to the vibrational modes of the initial state peaks. The peak at 3583 cm^{-1} corresponds to the stretching vibration of H24-O23 in the initial state, while the peak at 1970 cm^{-1} corresponds to the stretching vibration of H24-O23 in the transition state.

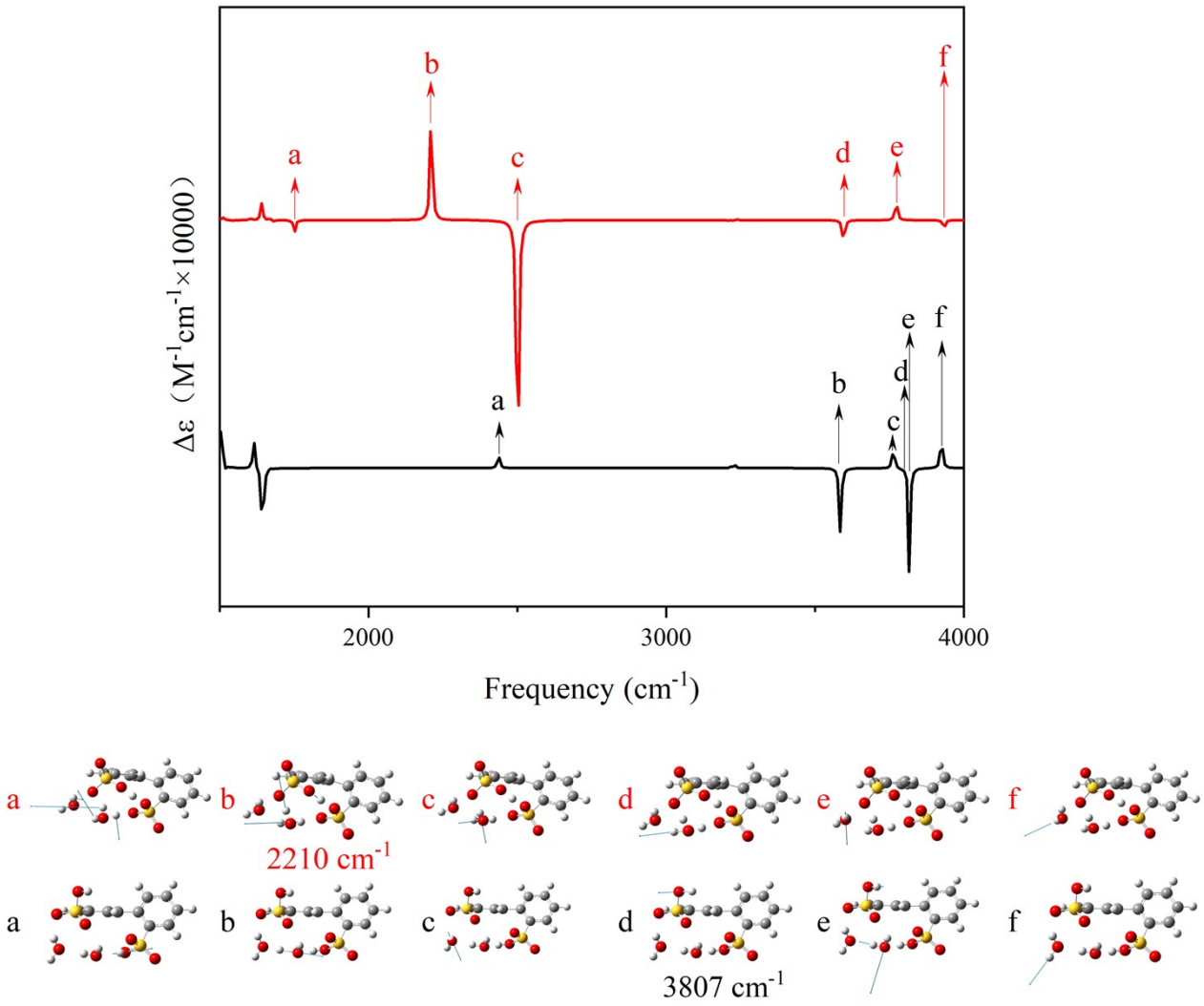

Supplementary Figure S11|Vibrational Circular Dichroism spectroscopy of BPD-2W. Black lines represent the ground state, and red lines represent the proton transition state. The red a and b correspond to the vibrational modes of the transition state peaks, while the black a and b correspond to the vibrational modes of the initial state peaks. The peak at 3807 cm^{-1} corresponds to the stretching vibration of H24-O23 in the initial state, while the peak at 2210 cm^{-1} corresponds to the stretching vibration of H24-O23 in the transition state.

5.Infrared spectroscopy

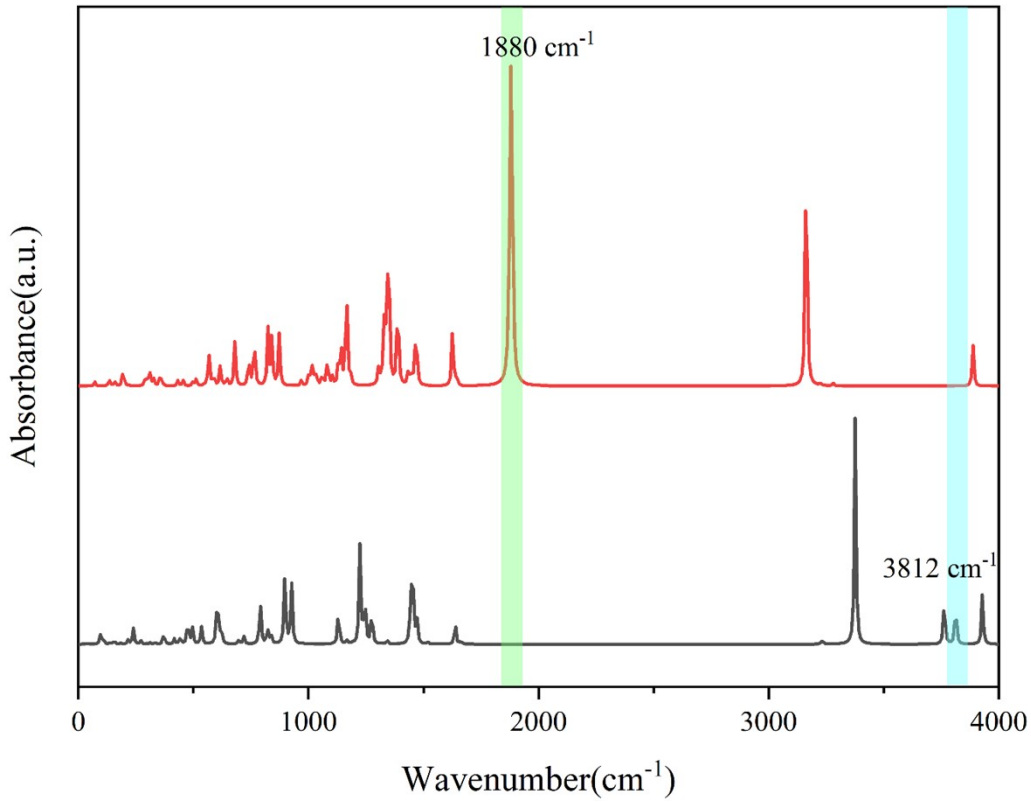

Supplementary Figure S12| Infrared spectroscopy of MBS-1W. Black lines represent the ground state, and red lines represent the proton transition state. The blue line corresponds to the characteristic peaks of the ground-state H20, while the green line corresponds to those of the excited-state H20.

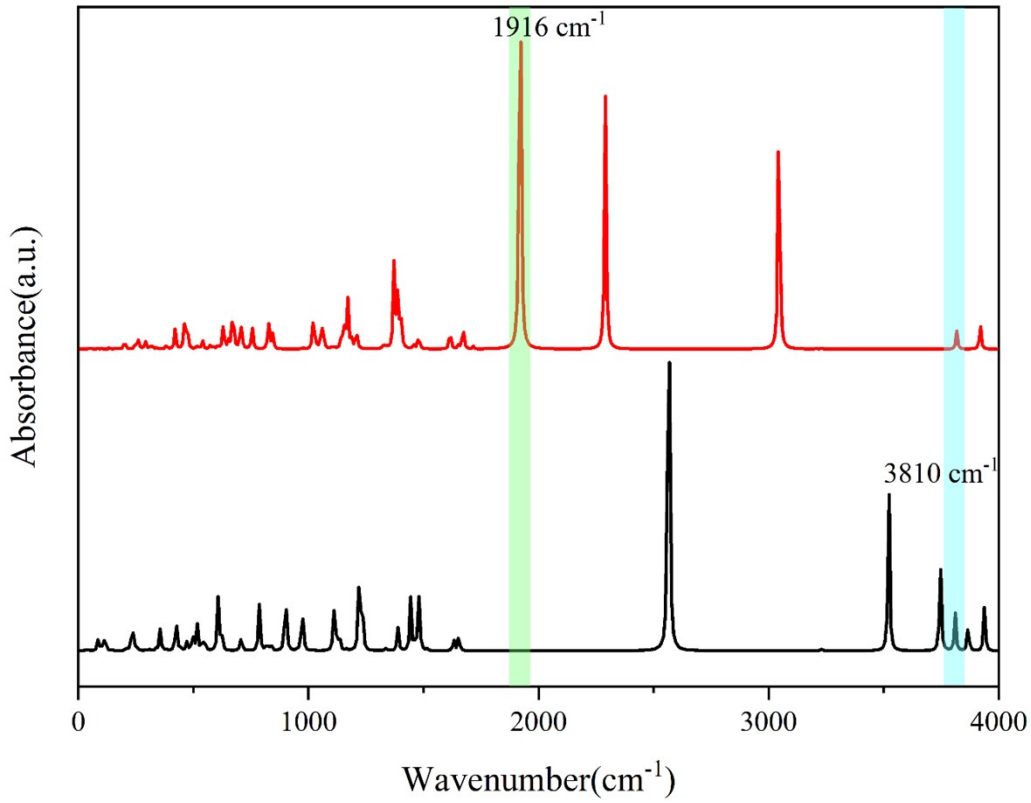

Supplementary Figure S13| Infrared spectroscopy of MBS-2W. Black lines represent the ground state, and red lines represent the proton transition state. The blue line corresponds to the characteristic peaks of the ground-state H20, while the green line corresponds to those of the excited-state H20.

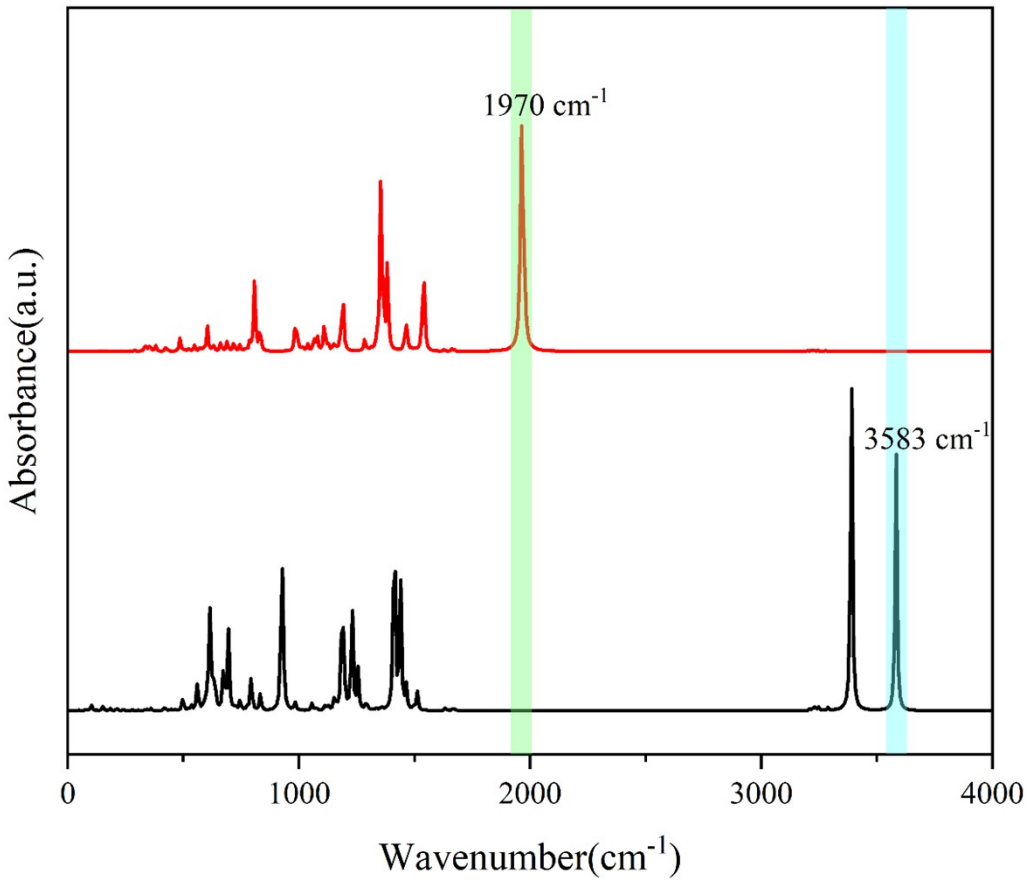

Supplementary Figure S14| Infrared spectroscopy of BPD-0W. Black lines represent the ground state, and red lines represent the proton transition state. The blue line corresponds to the characteristic peaks of the ground-state H24, while the green line corresponds to those of the excited-state H24.

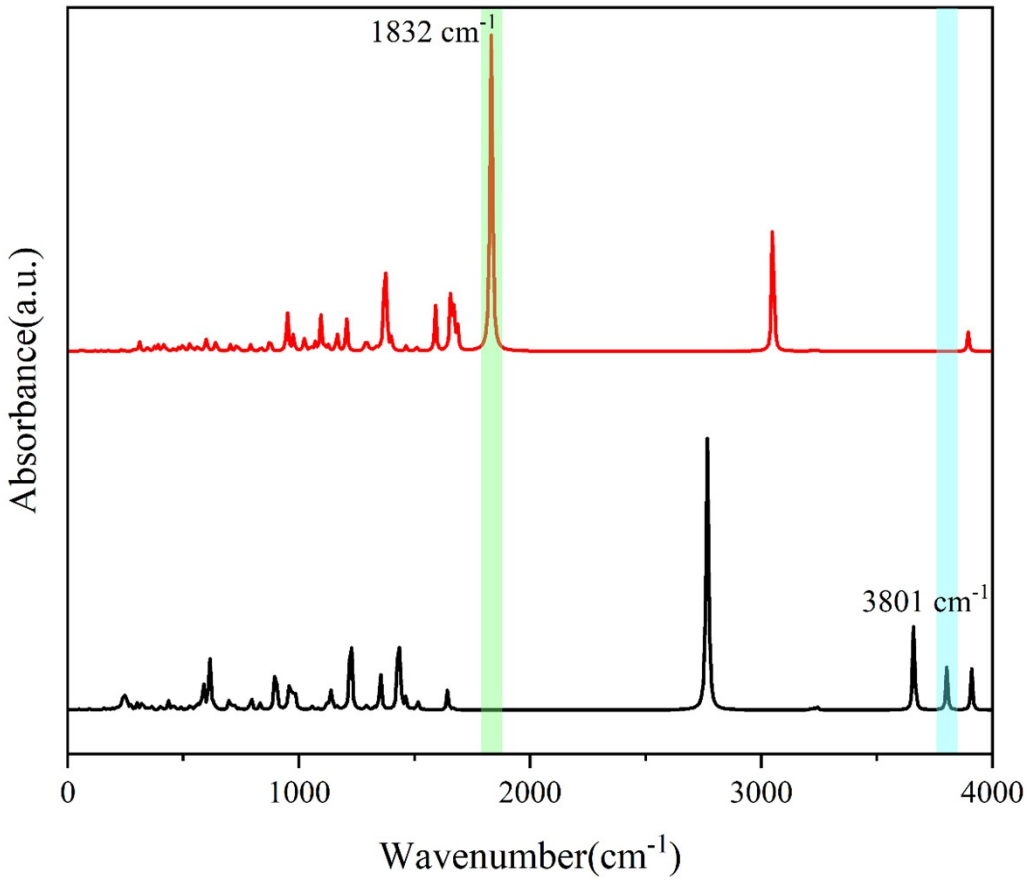

Supplementary Figure S15| Infrared spectroscopy of BPD-1W. Black lines represent the ground state, and red lines represent the proton transition state. The blue line corresponds to the characteristic peaks of the ground-state H24, while the green line corresponds to those of the excited-state H24.

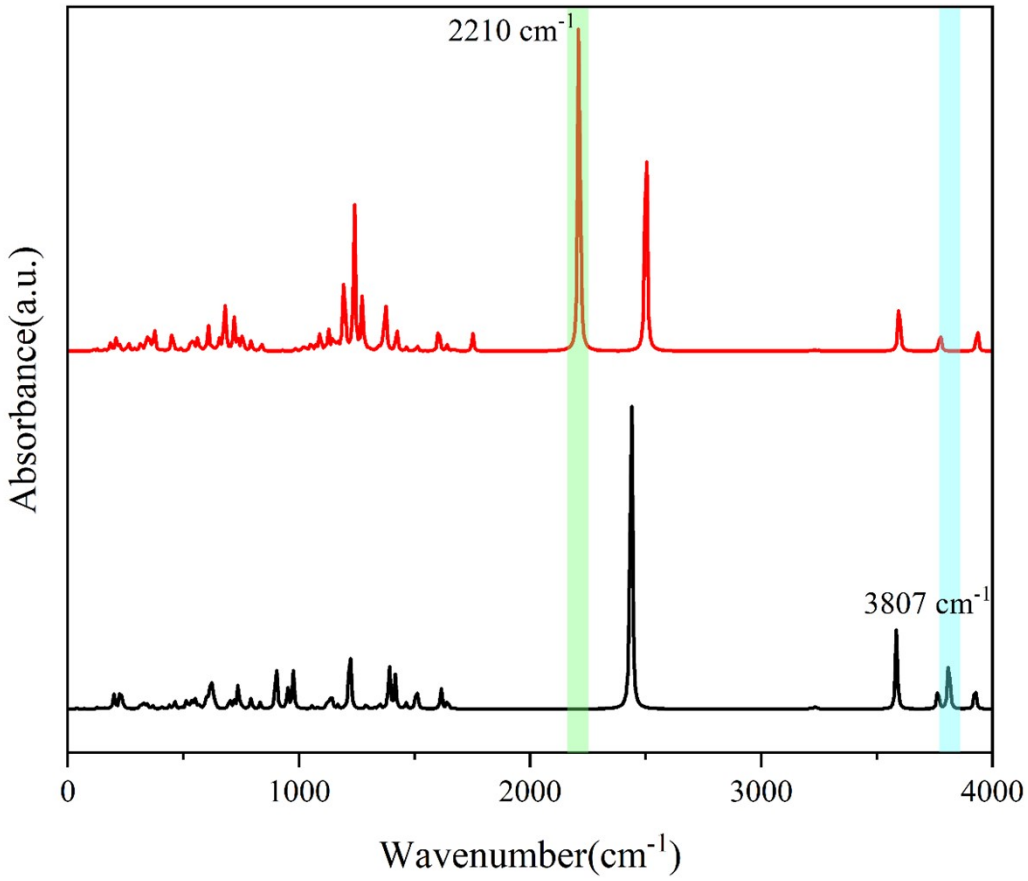

Supplementary Figure S16| Infrared spectroscopy of BPD-2W. Black lines represent the ground state, and red lines represent the proton transition state. The blue line corresponds to the characteristic peaks of the ground-state H24, while the green line corresponds to those of the excited-state H24.

6.Raman spectroscopy

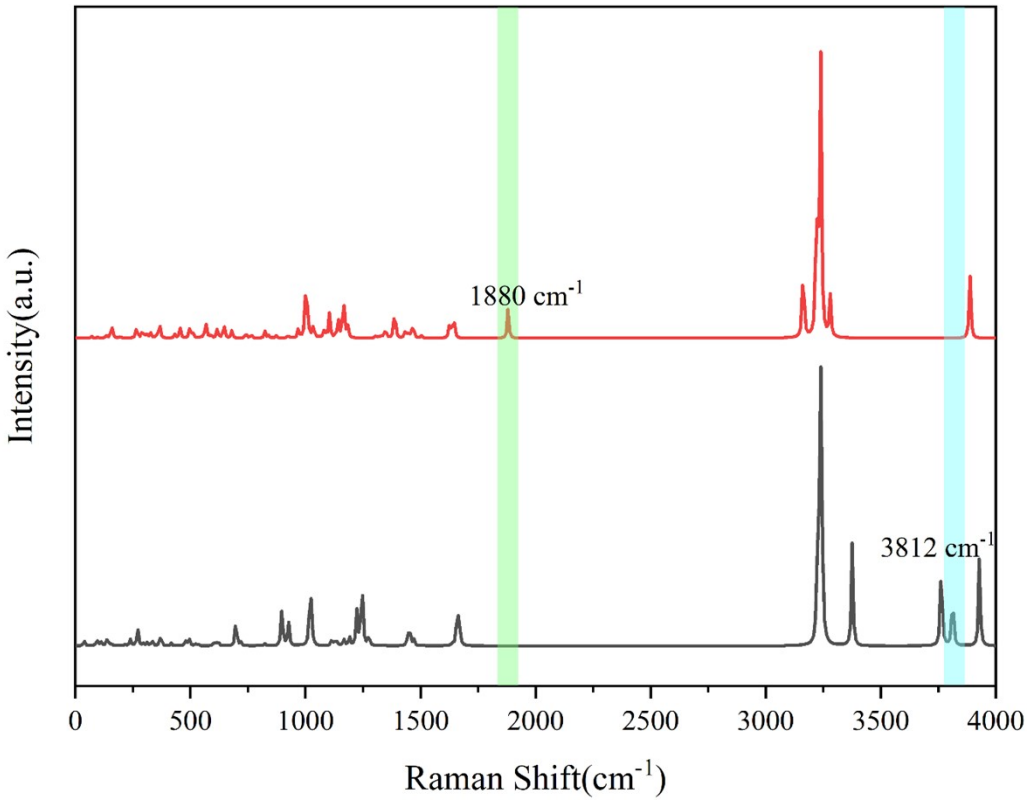

Supplementary Figure S17| Raman spectroscopy of MBS-1W. Black lines represent the ground state, and red lines represent the proton transition state. The blue line corresponds to the characteristic peaks of the ground-state H20, while the green line corresponds to those of the excited-state H20.

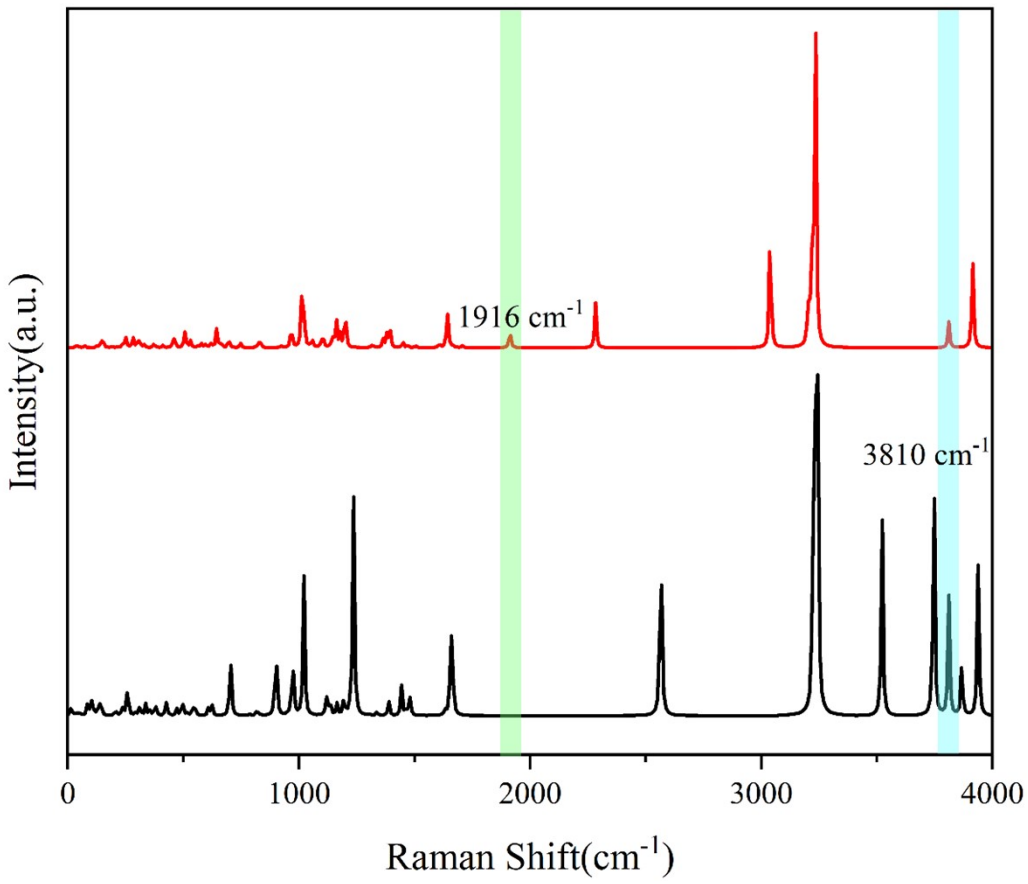

Supplementary Figure S18| Raman spectroscopy of MBS-2W. Black lines represent the ground state, and red lines represent the proton transition state. The blue line corresponds to the characteristic peaks of the ground-state H20, while the green line corresponds to those of the excited-state H20.

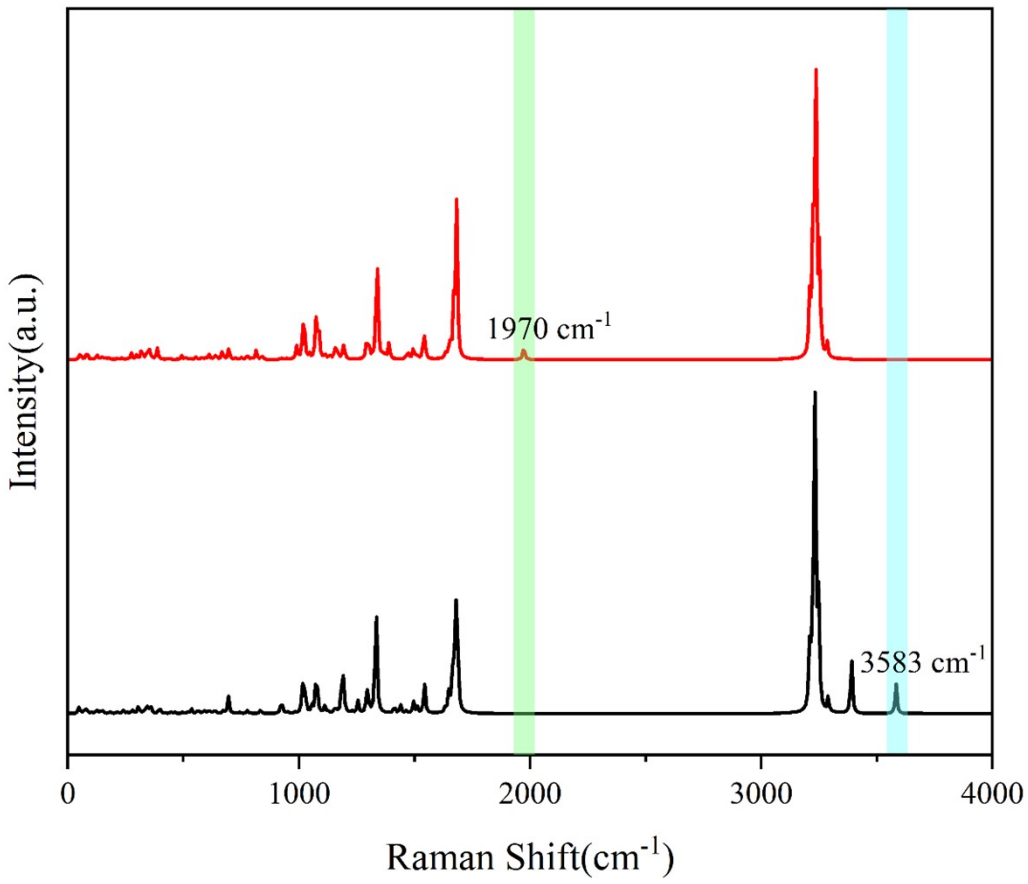

Supplementary Figure S19| Raman spectroscopy of BPD-0W. Black lines represent the ground state, and red lines represent the proton transition state. The blue line corresponds to the characteristic peaks of the ground-state H24, while the green line corresponds to those of the excited-state H24.

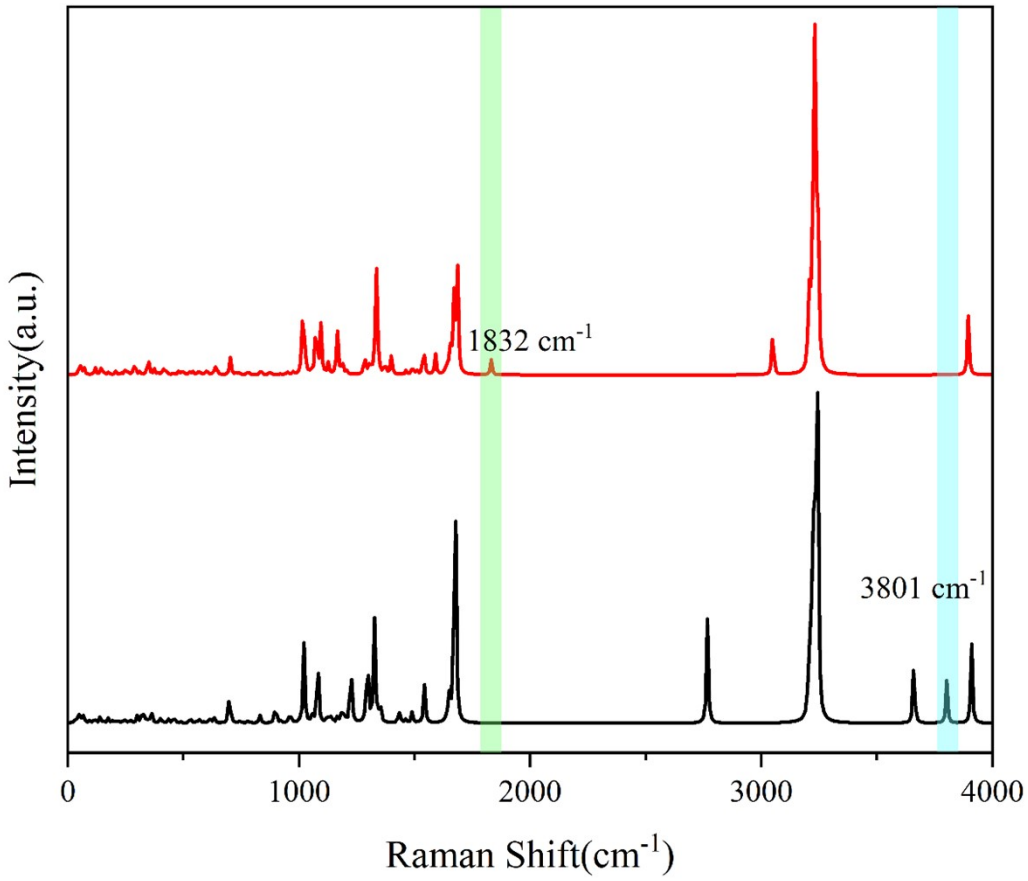

Supplementary Figure S20| Raman spectroscopy of BPD-1W. Black lines represent the ground state, and red lines represent the proton transition state. The blue line corresponds to the characteristic peaks of the ground-state H24, while the green line corresponds to those of the excited-state H24.

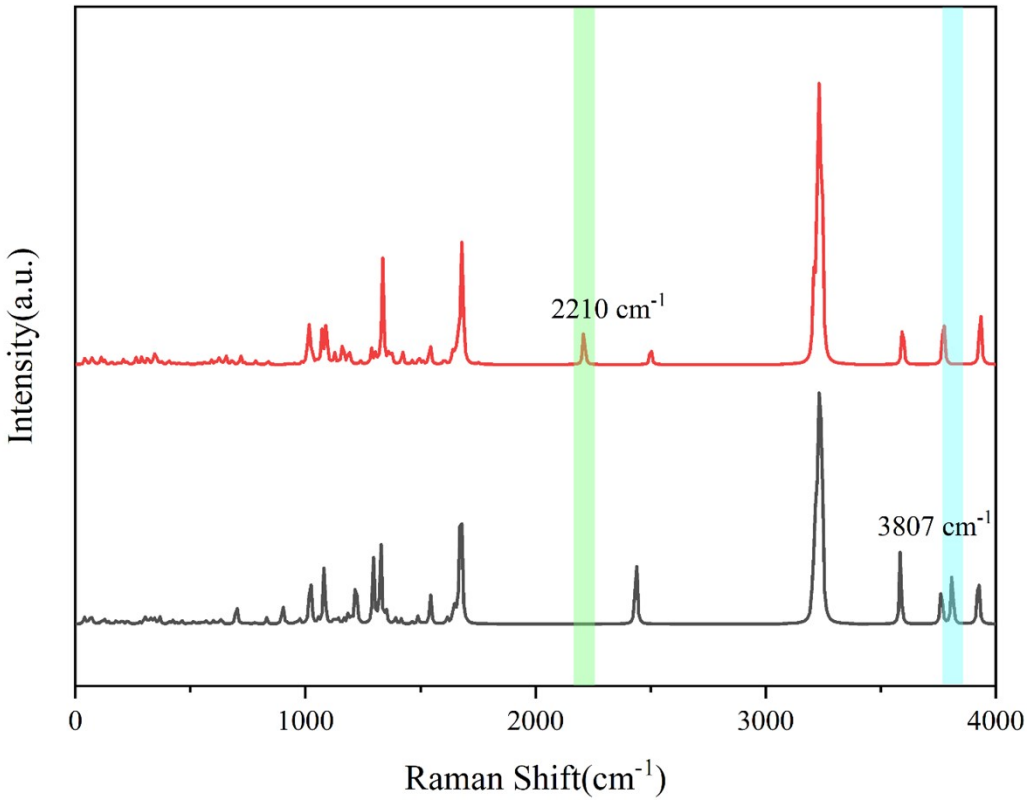

Supplementary Figure S21| Raman spectroscopy of BPD-2W. Black lines represent the ground state, and red lines represent the proton transition state. The blue line corresponds to the characteristic peaks of the ground-state H24, while the green line corresponds to those of the excited-state H24.

7.Ultraviolet-Visible Absorption Spectrum

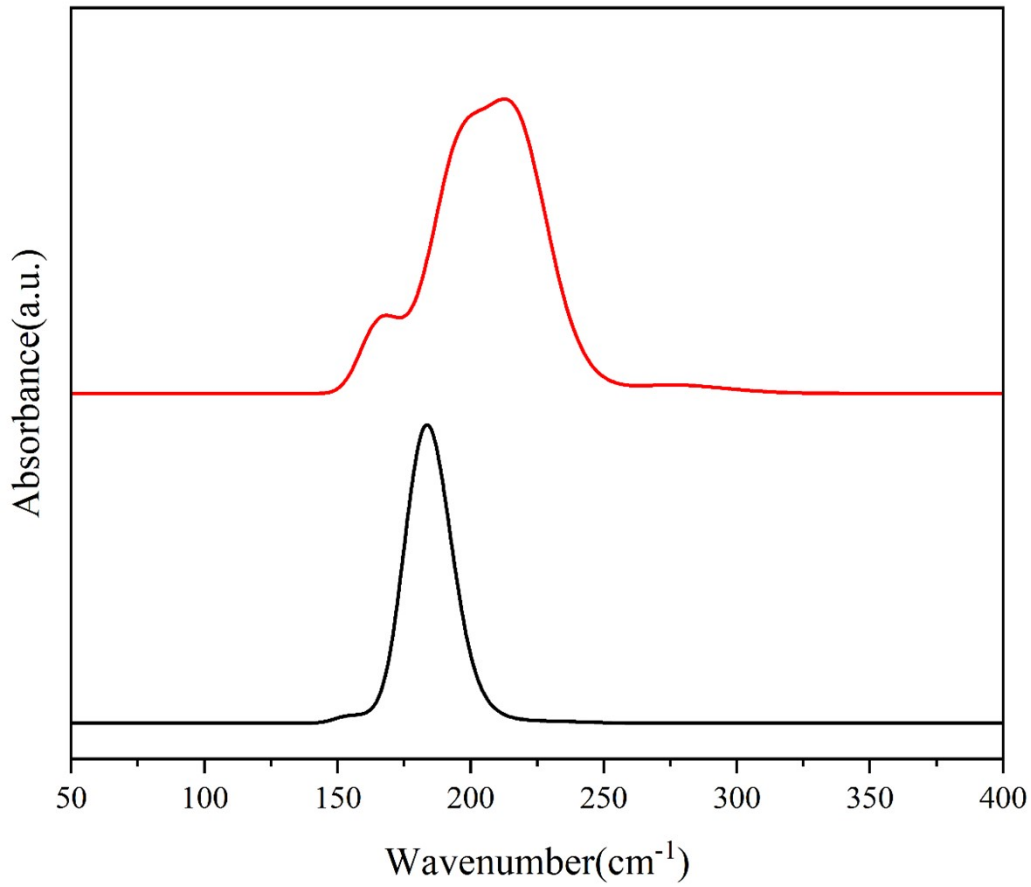

Supplementary Figure S22| Ultraviolet-Visible Absorption Spectrum of MBS-1W. Black lines represent the ground state, and red lines represent the proton transition state.

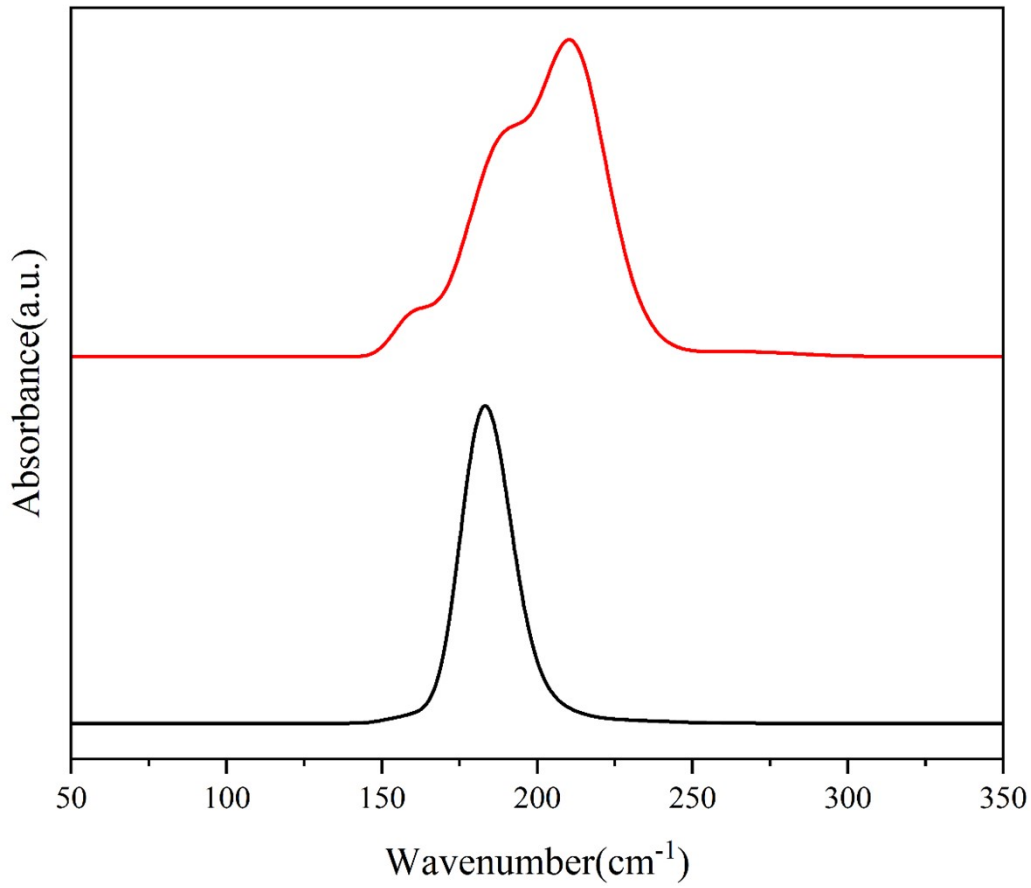

Supplementary Figure S23| Ultraviolet-Visible Absorption Spectrum of MBS-2W. Black lines represent the ground state, and red lines represent the proton transition state.

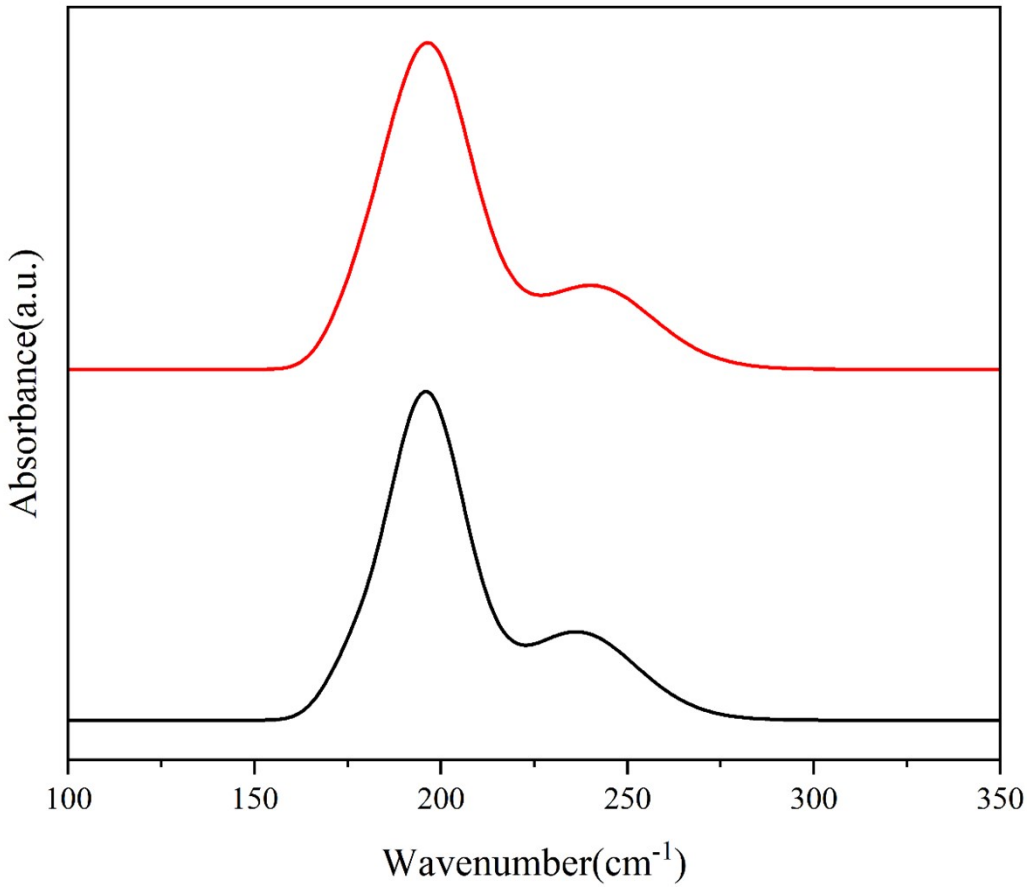

Supplementary Figure S24| Ultraviolet-Visible Absorption Spectrum of BPD-0W. Black lines represent the ground state, and red lines represent the proton transition state.

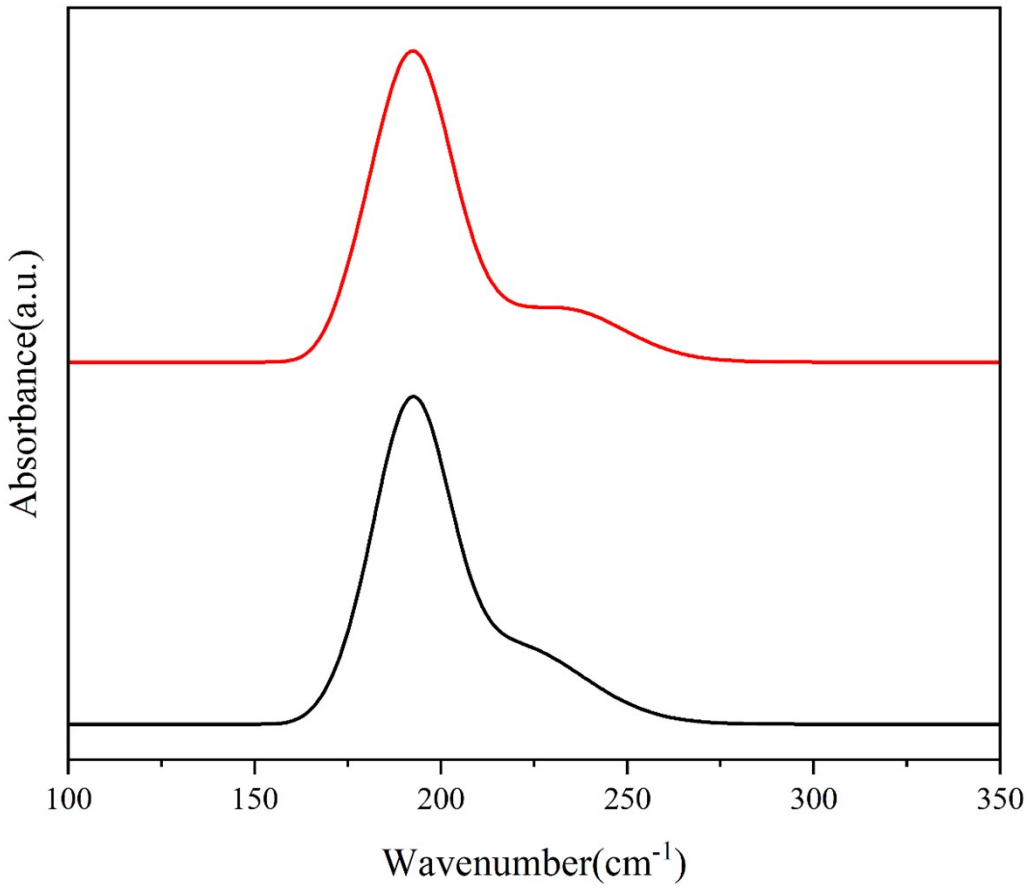

Supplementary Figure S25| Ultraviolet-Visible Absorption Spectrum of BPD-1W. Black lines represent the ground state, and red lines represent the proton transition state.

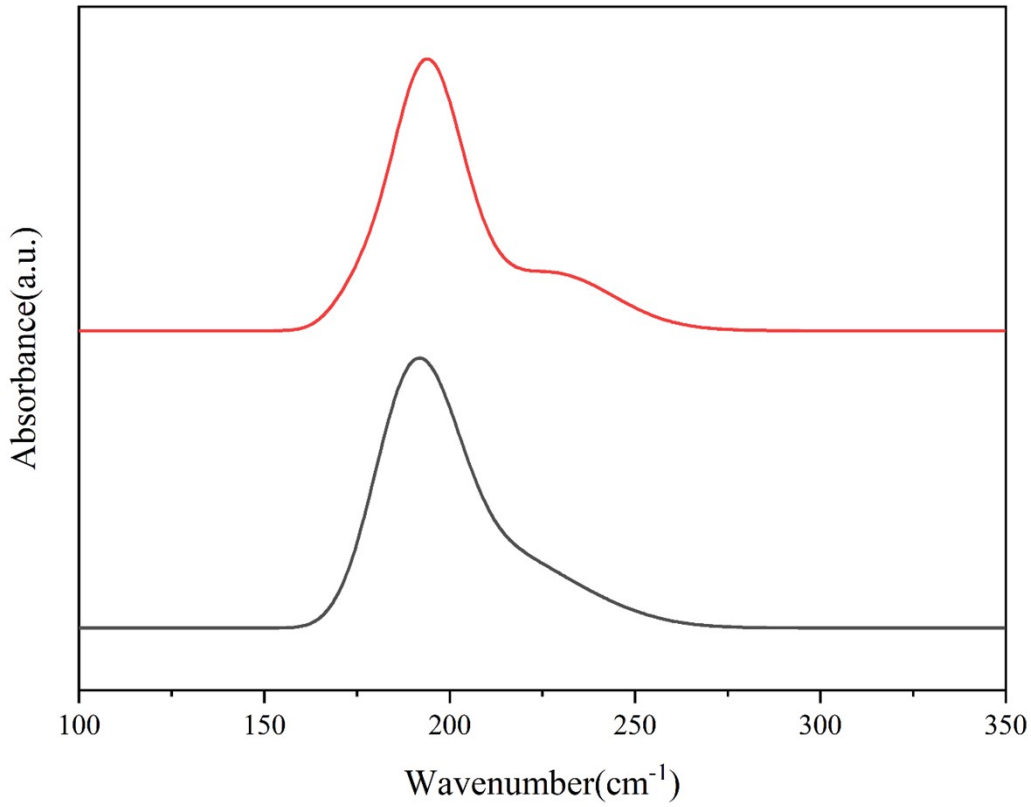

Supplementary Figure S26| Ultraviolet-Visible Absorption Spectrum of BPD-2W. Black lines represent the ground state, and red lines represent the proton transition state.

8.^{1}H-NMR spectra

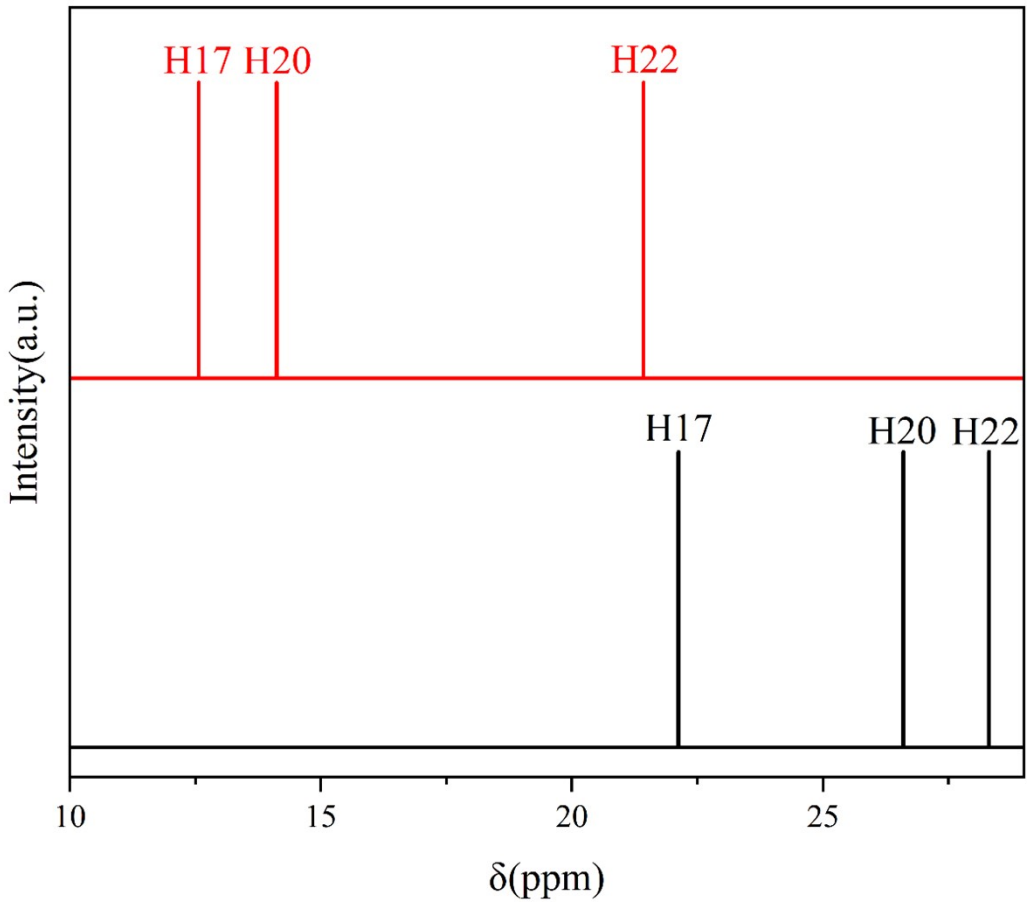

Supplementary Figure S27| ^{1}H-NMR spectrum of MBS-1W. Black lines represent the ground state, and red lines represent the proton transition state.

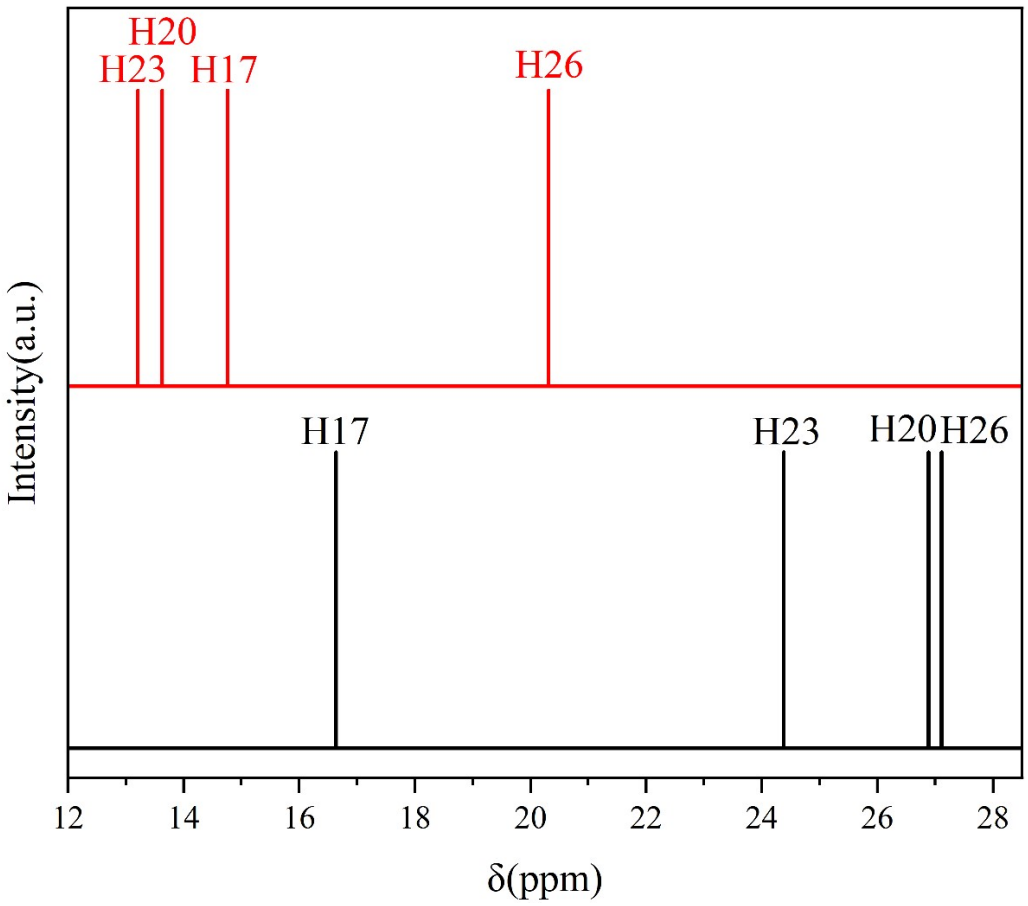

Supplementary Figure S28| ^{1}H-NMR spectrum of MBS-2W. Black lines represent the ground state, and red lines represent the proton transition state.

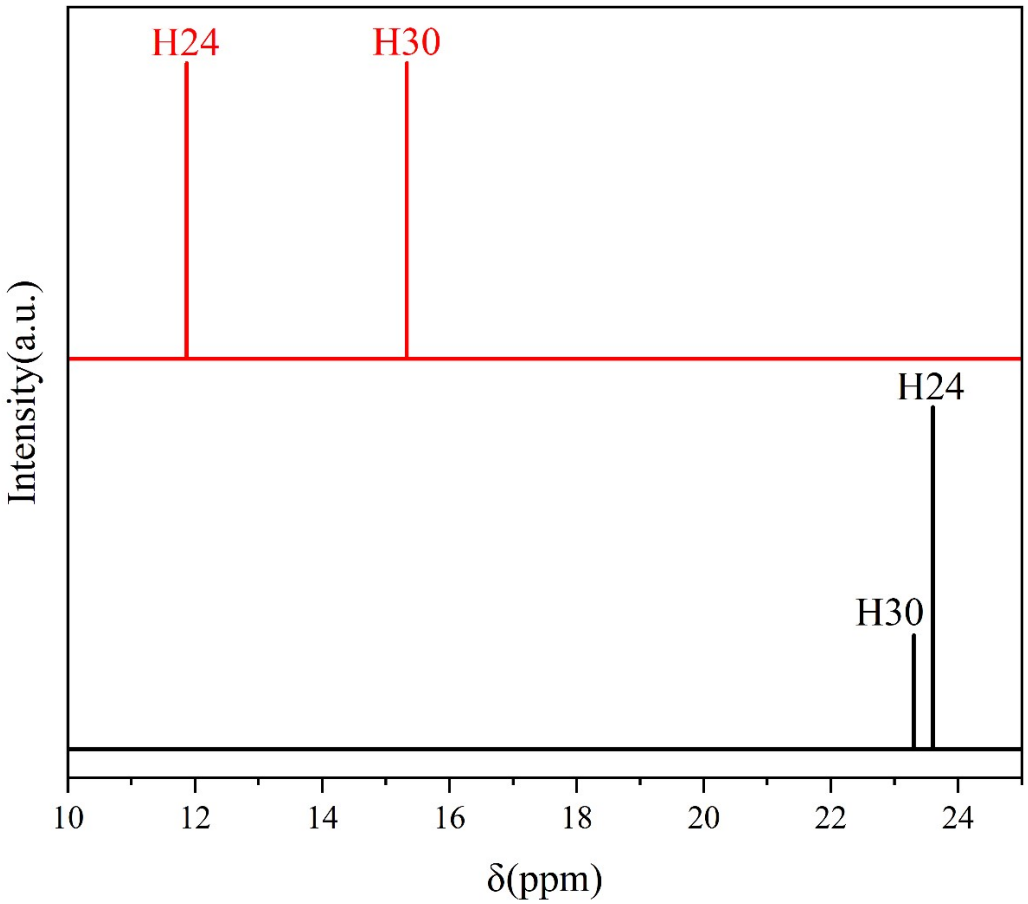

Supplementary Figure S29| ^{1}H-NMR spectrum of BPD-0W. Black lines represent the ground state, and red lines represent the proton transition state.

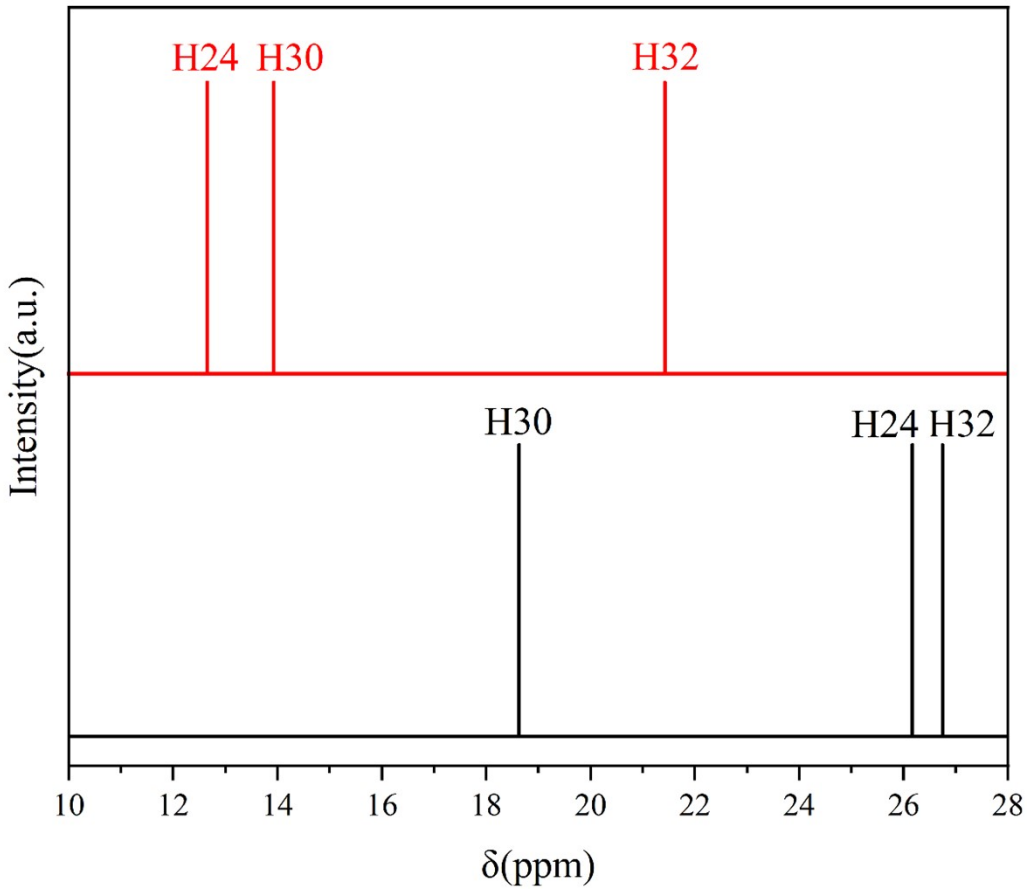

Supplementary Figure S30| ^{1}H-NMR spectrum of BPD-1W. Black lines represent the ground state, and red lines represent the proton transition state.

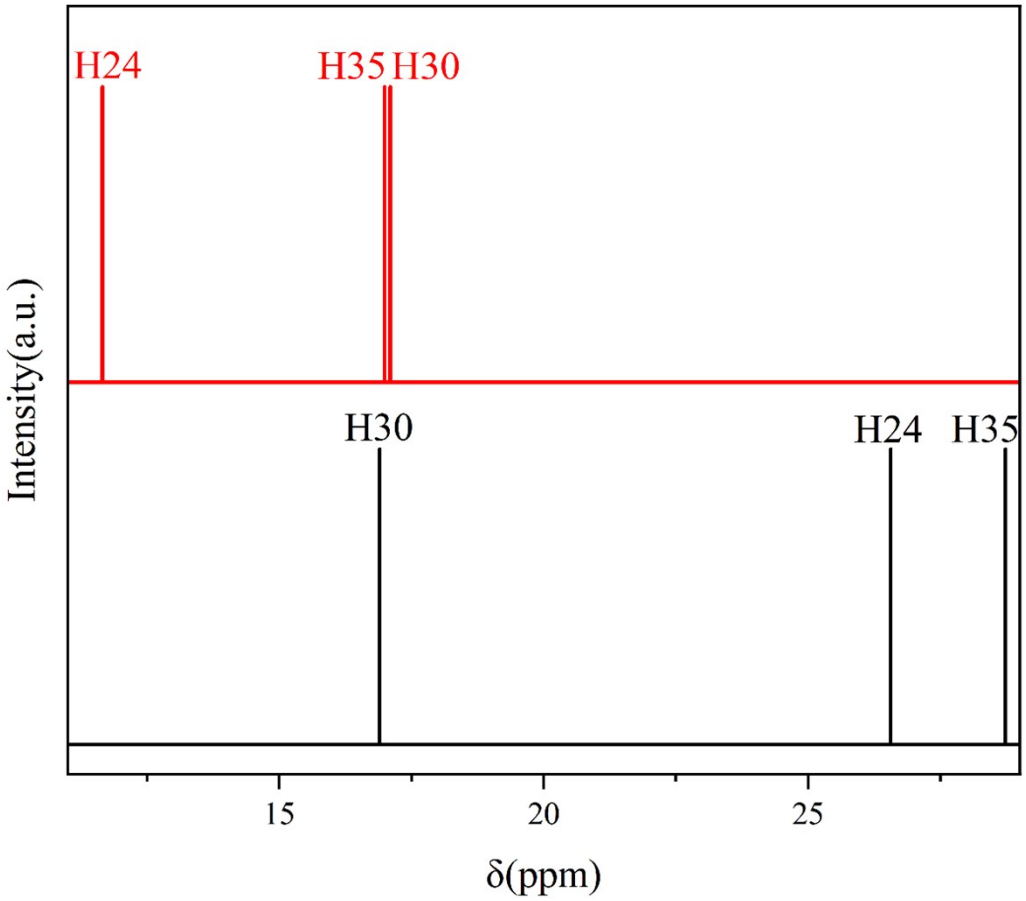

Supplementary Figure S31| ^{1}H-NMR spectrum of BPD-2W. Black lines represent the ground state, and red lines represent the proton transition state.